Robust Vibration Attenuation for Autonomous Robotic Observation Systems

Fatemeh Rekabi-Bana [*,1] **Mahmood Saadat** [*]
Martin Stefanec [***] **Tomáš Vintr** [*] **Honghao Pan** [*]
Mohsen Zahmatkesh [*] **Tomáš Krajník** [**] **Thomas Schmickl** [***]
Farshad Arvin [*]

[*] *Department of Computer Science, Durham University*
[**] *Artificial Intelligence Centre, FEE, Czech Technical University*
[***] *Department of Zoology, Institute of Biology, University of Graz*

Abstract: Advanced behavioural studies for social insects such as honeybees demand high-precision mechatronic systems to perform uninterrupted observations. This paper proposes a robust framework to attenuate the vibration generated by the mechatronic part of the Autonomous Robotic Observation and Behavioural Analysis (AROBA) system. The vibration attenuation method proposed in this paper incorporates the output feedback H_∞ approach for input shaping of the acceleration commands to the drive system. The controller is designed based on the state space system identification results for an unknown order linear time-invariant (LTI) model. The output feedback H_∞ is applied to compensate for the modelling uncertainties while regulating the vibration. The results showcase the robust performance obtained from the experiments with the AROBA mechatronic system. The closed-loop system achieved an average vibration signal power below -60 dB which is significantly lower than the value that is not disturbing the bees' behaviour according to the studies in this field.

Keywords: Robotic observation, Output feedback H_∞, System Identification, Vibration control,

1. INTRODUCTION

Recent advancements in robotics open new ways for robot-insect interaction according to Ulrich et al. (2024); Janota et al. (2024). However, Romano et al. (2019, 2024) showed that robot-animal interaction demands resolving many challenges. According to Stefanec et al. (2022); Barmak et al. (2023), robotic technology can transform such biological studies as the robots can observe insects in their natural habitat continuously and determine their collective behaviour. For a continuous behavioural analysis, a novel robotic system was introduced in Rekabi-Bana et al. (2023); Ulrich et al. (2024); Blaha et al. (2024), which is an observation and interaction mechanism for long-term studies on honeybee colonies. In addition to the criteria for structural service life, according to Stefanec et al. (2021), the biological experiment demands reducing the vibration level as honeybees react to the vibration transferred to the hive. Based on previous studies such as Hrncir et al. (2019), if the transferred vibration intensity in the frequency range of 0 to 50 Hz is prominent, it might interfere with the honeybee's behaviour. For instance, one of the communications that honeybees show is the waggle dance, which has an average frequency of 14.6 Hz based on Łopuch and Tofilski (2017). Therefore, the mechatronic system must attenuate the generated vibration between 10 Hz and 20 Hz significantly. Although the implemented passive vibration absorption technique in Ulrich et al. (2024) reduces the vibration significantly, an active method enhances the vibration attenuation for biological experiments, structural health, and image quality (Žampachů et al., 2022). On the other hand, a feed drive mechanism needs sophisticated control methods to attenuate the vibration while following the desired position and velocity commands based on Yang et al. (2020); Balaji and Karthik Selva Kumar (2021); Lu et al. (2018). Although recent studies such as Zhu et al. (2016) introduce different approaches to identify appropriate models, particularly for the ballscrew systems, based on nonlinear approaches presented in Liu et al. (2023) or evolutionary optimisation demonstrated in Li et al. (2023), those algorithms cannot encounter the effect of other parts such as supporting units, joints, or housings in the resulting vibration. On the other hand, the control methods that are applicable for dissipating the vibration, such as H_2 synthesis controller for damping enhancement presented in Shirvani et al. (2022), the linear quadratic regulator for high bandwidth control presented in Dumanli and Sencer (2018), and the μ synthesis controller proposed in Zhu et al. (2023) rely on accurate linear time-invariant models that describe the system's behaviour. Therefore, the vibration control performance depends not only on the control algorithm but also on the model's accuracy utilised for the control design process as described in Rekabi-Bana et al. (2024). This paper proposes a new control framework to address the uncertain model obtained from system identification. The proposed framework comprises

[1] Corresponding author. Fatemeh Rekabi-Bana, fatemeh.rekabi-bana@durham.ac.uk
This work was supported by EU H2020-FET-OPEN RoboRoyale project [grant number 964492]

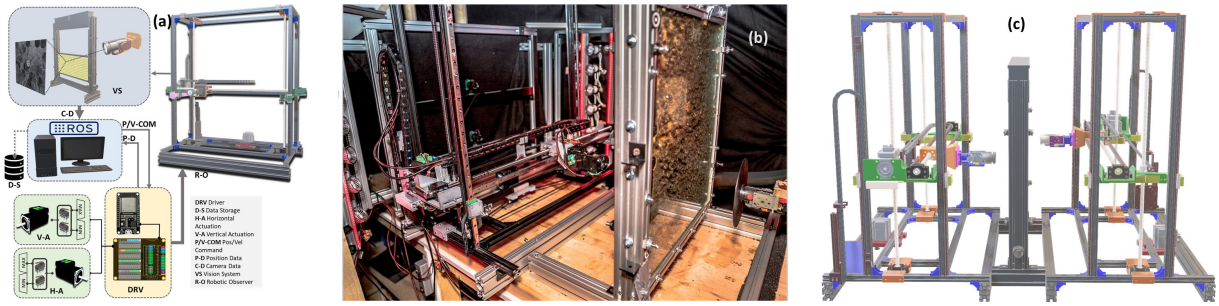

Fig. 1. The autonomous observation system collects the queen honeybee's behavioural information. (a) The mechatronic system and its main components, (b) the mechatronic system in its real workspace with the observation hive, and (c) the CAD model of the experiments for data collection from the queen.

an output feedback H_∞ approach that employs an estimated Linear Time Invariant (LTI) model to determine an acceleration command for regulating the predicted vibrations (Yalçın and Erkan, 2021; Rekabi et al., 2020). On the other hand, to determine the LTI model for the controller design purpose, the unknown structured state space system identification approach is employed due to its capability for model order and parameter identification simultaneously, as demonstrated in Soares Jr and Serpa (2022). This method showcased its capability for modal analysis in different robotic applications and validated its performance for different dynamic systems such as those presented in Pappalardo et al. (2023). Therefore, the main contributions of this paper are as follows:

- Incorporating the Multivariable Output-Error State Space (MOESP) identification method that determines the LTI model to estimate the vibration generated by the mechatronic system according to the acceleration in both the horizontal and vertical axes.
- Development of a new robust control framework based on H_∞ method, which employs an uncertain LTI model to attenuate the vibration and compensate for the modelling uncertainties.

2. AUTONOMOUS OBSERVATION MECHANISM

The AROBA system comprises the mechanical design and development of a robust drive system for the actuation. The schematic diagram presented in Fig. 1 describes different components of the system and how they interact with each other to fulfil the objectives.

The mechanical system includes an aluminium frame, a ball screw feed drive system for vertical motion, and a horizontal linear actuation unit. As demonstrated in Fig. 1, the AROBA system has two cooperative robots that simultaneously cover two sides of the observation hive to track the queen and explore other events, such as larva growth in the cells. In this paper, an input shaping controller was developed to reduce the vibration generated as much as possible to capture high-quality images. That system is structured as follows:

- The state machine to switch between the acceleration, deceleration, and constant speed modes.
- A robust controller to regulate the vibration output of the system.

3. STATE MACHINE FOR THE DRIVER

The presented state machine in Algorithm. 1 was employed to apply variable acceleration in each working state. The state machine considers four states and the transition rules between those states.

Algorithm 1 Driver State Machine

while true: **do**
  State: Idle
  if $\Delta d \geq d_l$ **then** Condition to transition from Idle
    $v_{tgt} \leftarrow v_{cmd}$, **State:** Acceleration
  end if
  State: Acceleration
  if $\Delta d < D_{arv}$ **then** Transition to Deceleration
    $v_{tgt} \leftarrow 0$, **State:** Deceleration
  else if $|\Delta v| \leq v^l_{ths}$ **then State:** Constant Speed
  end if
  State: Constant Speed
  if $\Delta d < D_{arv}$ **then** Transition to Deceleration
    $v_{tgt} \leftarrow 0$, **State:** Deceleration
  else if $v_{tgt} \neq v_{cmd}$ **then State:** Acceleration
  end if
  State: Deceleration
  if $|v| \leq v^l_{ths}$ **then State**: Idle
  else if $\Delta d \geq 3D_{arv}$ **then** Transition to Acceleration
    $v_{tgt} \leftarrow v_{cmd}$, **State:** Acceleration
  end if
end while

In Algorithm. 1, $v \in \mathbb{R}$ stands for the velocity in each axis, $v_{tgt} \in \mathbb{R}$ is the target velocity, $v_{cmd} \in \mathbb{R}$ is the velocity command, $\Delta v = v - v_{tgt}$, $v^l_{ths} \in \mathbb{R}$ is the threshold level for the velocity error, $d_l \in \mathbb{R}$ is the dead zone level for the idle mode, $\Delta d \in \mathbb{R}$ is the distance to the position command, $D_{arv} \in \mathbb{R}$ is the arrival distance which is determined as $D_{arv} = \frac{1}{2}\frac{v^2}{a_{com}}$, where $a_{com} \in \mathbb{R}$ is the acceleration command.

4. SUBSPACE SYSTEM IDENTIFICATION FOR MODELING

The following linear state-space model is considered to describe the vibration generated by the mechanism.

$$\dot{\mathbf{x}} = \mathbf{A}\mathbf{x} + \mathbf{B}\mathbf{u}\ , \qquad (1)$$
$$\mathbf{y} = \mathbf{C}\mathbf{x} + \mathbf{D}\mathbf{u}\ ,$$

where $\mathbf{x} \in \mathbb{R}^n$ is the state vector, n represents the system's order, $\mathbf{u} = \begin{bmatrix} a^c_x & a^c_y \end{bmatrix} \in \mathbb{R}^2$ is the control vector and is

equivalent to the acceleration commands, which are stated as a_x^c and a_y^c. Also, $\mathbf{y} \in \mathbb{R}^3$ is the output vector and is equivalent to the vibration measurement in the x, y, and z directions at the sensor location. The state transition matrix $\mathbf{A} \in \mathbb{R}^{n\times n}$, the control transition matrix $\mathbf{B} \in \mathbb{R}^{n\times 2}$, the state observability matrix $\mathbf{C} \in \mathbb{R}^{3\times n}$ and $\mathbf{D} \in \mathbb{R}^{3\times 2}$ which represents the control signal's contribution to the observation are the matrices to describe the state space model in Eq. 1. This paper employs the MOESP algorithm to estimate the system's matrices based on the data collected from the experiments. According to Favoreel et al. (2000) and Van Overschee and De Moor (1994), the following equation estimates the system matrices based on the inputs and outputs collected from the experiment:

$$\underset{\hat{\mathbf{A}},\hat{\mathbf{B}},\hat{\mathbf{C}},\hat{\mathbf{D}}}{\mathbf{argmin}} \left\| \begin{bmatrix} \mathbf{\Gamma}_{i-1}^{\dagger}\mathbf{Z_{i+1}} \\ \mathbf{Y}_{i|i} \end{bmatrix} - \begin{bmatrix} \hat{\mathbf{A}} & \hat{\mathbf{B}} \\ \hat{\mathbf{C}} & \hat{\mathbf{D}} \end{bmatrix} \begin{bmatrix} \mathbf{\Gamma}_{i}^{\dagger}\mathbf{Z_i} \\ \mathbf{U}_{i|2i-1} \end{bmatrix} \right\| , \tag{2}$$

where, $\hat{[.]}$ represent the estimated value of the argument, $[.]^{\dagger}$ demonstrates the Moore-Penrose Pseudo inverse operator. The block Hankel matrices $\mathbf{Y}_{k|t}$ and $\mathbf{U}_{k|t}$ determine the measurement and input matrices between the time steps k and t. Also, $\mathbf{Z}_i$ is the projection matrix defined according to the following equations:

$$\mathbf{Z}_i = \mathbf{Y}_{i|2i-1}\mathbf{S}_i'(\mathbf{S}_i\mathbf{S}_i')^{-1}\mathbf{S}_i \ , \ \mathbf{S}_i = \begin{bmatrix} \mathbf{U}_{0|i-1} \\ \mathbf{U}_{i|2i-1} \\ \mathbf{Y}_{0|i-1} \end{bmatrix} , \tag{3}$$

where $[.]'$ represents the transpose of the matrix. Furthermore, the matrix $\mathbf{\Gamma}_i$ which is the extended observability matrix and is equivalent to $\mathbf{\Lambda}_1\mathbf{\Sigma}_1^{\frac{1}{2}}$ where the matrices $\mathbf{\Lambda}_1$ and $\mathbf{\Sigma}_1$ are determined from the singular value decomposition as follows:

$$\begin{aligned} &\begin{bmatrix} \mathbf{L}_i^1 & \mathbf{L}_i^3 \end{bmatrix} \begin{bmatrix} \mathbf{U}_{0|i-1} \\ \mathbf{Y}_{0|i-1} \end{bmatrix} = \begin{bmatrix} \mathbf{\Lambda}_1 & \mathbf{\Lambda}_2 \end{bmatrix} \begin{bmatrix} \mathbf{\Sigma}_1 & [\mathbf{0}] \\ [\mathbf{0}] & [\varepsilon] \end{bmatrix} \mathbf{V}' \ , \\ &\begin{bmatrix} \mathbf{L}_i^1 & \mathbf{L}_i^2 & \mathbf{L}_i^3 \end{bmatrix} = \mathbf{Z}_i\mathbf{S}_i^{\dagger} \ , \\ &\mathbf{L}_i^1 \in \mathbb{R}^{li\times mi}, \ \mathbf{L}_i^2 \in \mathbb{R}^{li\times mi}, \ \mathbf{L}_i^1 \in \mathbb{R}^{li\times li} \ , \end{aligned} \tag{4}$$

where $[\varepsilon]$ represents the singular values that are insignificant compared to other elements in $\mathbf{\Sigma}_1$. Therefore, the main role of $\mathbf{\Sigma}_1$ in the identification process is to determine the system's order according to the variations in singular values. Accordingly, Eq. 2 can be solved considering the model's order identified in Eq. 4 and applying the numerical methods presented in Van Overschee and De Moor (1994) to determine the system matrices.

To obtain the best results for system identification, the input signal should excite the structure properly and make outputs that can be processed by Eq. 3 and Eq. 4. Therefore, the following characteristics are considered to generate the input signals for better excitation:

- A square signal with a constant amplitude and a duration from a uniform distribution between 0.1 s and 10 s.
- The time of action for each command is selected randomly.

The generated signal is the acceleration input to the state machine, and the position and velocity inputs are determined according to the acceleration input integration. The block Hankel matrices in Eq. 3 and Eq. 4 are determined based on the acceleration input signal to estimate a consistent model for the system, which includes the effect of the state machine with all nonlinear actions such as saturation, dead zone, and rate limits.

5. H_∞ CONTROLLER DESIGN

Considering the Linear Time Invariant (LTI) model for the system and employing the estimated matrices in the previous section in Eq. 1 causes modelling uncertainties that should be compensated by an appropriate control method. Therefore, the uncertain model can be described as follows:

$$\begin{aligned} \dot{\mathbf{x}} &= \hat{\mathbf{A}}\mathbf{x} + \hat{\mathbf{B}}\mathbf{u} + \mathbf{w}, \\ \mathbf{y} &= \hat{\mathbf{C}}\mathbf{x} + \hat{\mathbf{D}}\mathbf{u}, \\ \boldsymbol{\xi} &= \mathbf{H}(\mathbf{x},\mathbf{u}), \end{aligned} \tag{5}$$

Where $\mathbf{w} \in \mathbb{R}^n$ is the vector that describes the effect of uncertainties in the state space model, $\boldsymbol{\xi} \in \mathbb{R}^n$ is the objective vector, and $\mathbf{H} \in \mathbb{R}^{n\times n}$ is the objective function where $\mathbf{H}'\mathbf{H} = \mathbf{x}'\mathbf{Q}\mathbf{x} + \mathbf{u}'\mathbf{R}\mathbf{u}$ and $\mathbf{Q} \geq 0$, $\mathbf{R} > 0$ are the state and control weight matrices which are symmetric. According to Eq. 5, the controller should stabilise the system around the origin $\mathbf{x} = 0$ and meanwhile attenuate the effect of uncertainties on the objective function. Therefore, for a positive value $0 < \gamma < 1$, the following equation should be satisfied to achieve the robust performance for the system described in Eq. 5:

$$\int_0^T \boldsymbol{\xi}'(t)\boldsymbol{\xi}(t)dt \leq \gamma^2 \int_0^T \mathbf{w}'(t)\mathbf{w}(t)dt, \tag{6}$$

According to Isidori and Astolfi (1992), the following conditions should be established to achieve Eq. 6 with the measurement feedback controller $\mathbf{u}$ for Eq. 5.

(I)-There exists $V(\mathbf{x}) > 0, \mathbf{x} \neq 0$ which is a smooth, positive definite function, and locally defined in a neighbourhood of the origin in $\mathbb{R}^n$, which satisfies the Hamilton-Jaccobi-Isaacs equation as follows:

$$\begin{aligned} &V_x'\hat{\mathbf{A}}\mathbf{x} - \gamma^2\boldsymbol{\alpha}_1'(\mathbf{x})\boldsymbol{\alpha}_1(\mathbf{x}) + \boldsymbol{\alpha}_2'(\mathbf{x})\mathbf{R}\boldsymbol{\alpha}_2(\mathbf{x}) + \mathbf{x}'\mathbf{Q}\mathbf{x} = 0 \ , \\ &\boldsymbol{\alpha}_1(\mathbf{x}) = \frac{1}{2\gamma^2}V_x, \ \boldsymbol{\alpha}_2(\mathbf{x}) = -\frac{1}{2}\mathbf{R}^{-1}\hat{\mathbf{B}}'V_x, \end{aligned} \tag{7}$$

where $V_x = \frac{\partial V}{\partial \mathbf{x}}$.

(II)- There exists a matrix $\mathbf{G} \in \mathbb{R}^{n\times 3}$, such that the equilibrium point $\boldsymbol{\zeta} = 0 \in \mathbb{R}^n$ of the following system is locally asymptotically stable.

$$\dot{\boldsymbol{\zeta}} = \hat{\mathbf{A}}\boldsymbol{\zeta} + \boldsymbol{\alpha}_1(\boldsymbol{\zeta}) - \mathbf{G}\hat{\mathbf{C}}\boldsymbol{\zeta} \ . \tag{8}$$

(III)- There exists a function $W(\mathbf{x},\zeta) \geq 0$ which is smooth, positive semidefinite, and locally defined in a neighbourhood of the origin in $\mathbb{R}^{n\times n}$ and such that $W(0,\zeta) > 0$ for each $\zeta \neq 0$, which solves the Hamilton-Jacobi equation stated as follows:

$$\begin{aligned} \begin{bmatrix} W_x' & W_\zeta' \end{bmatrix} f_e(\mathbf{x},\zeta) + h_e(\mathbf{x},\boldsymbol{\zeta})'h_e(\mathbf{x},\boldsymbol{\zeta}) \\ + \gamma^2\Phi'(\mathbf{x},\boldsymbol{\zeta})\Phi(\mathbf{x},\boldsymbol{\zeta}) = 0, \end{aligned} \tag{9}$$

where $W_x = \frac{\partial W}{\partial \mathbf{x}}$ and $W_\zeta = \frac{\partial W}{\partial \boldsymbol{\zeta}}$. Also, the functions $f_e(\mathbf{x},\zeta)$, $h_e(\mathbf{x},\zeta)$, and $\Phi(\mathbf{x},\zeta)$ are described as follows:

$$\begin{aligned} f_e(\mathbf{x},\zeta) &= \begin{bmatrix} \hat{\mathbf{A}}\mathbf{x} + \boldsymbol{\alpha}_1(\mathbf{x}) + \hat{\mathbf{B}}\boldsymbol{\alpha}_2(\zeta) \\ \hat{\mathbf{A}}\boldsymbol{\zeta} + \boldsymbol{\alpha}_1(\boldsymbol{\zeta}) + \hat{\mathbf{B}}\boldsymbol{\alpha}_2(\boldsymbol{\zeta}) + \mathbf{G}\hat{\mathbf{C}}(\mathbf{x}-\boldsymbol{\zeta}) \end{bmatrix}, \\ h_e(\mathbf{x},\boldsymbol{\zeta}) &= \boldsymbol{\alpha}_2(\boldsymbol{\zeta}) - \boldsymbol{\alpha}_2(\mathbf{x}), \Phi(\mathbf{x},\zeta) = \frac{1}{2\gamma^2}W_x' \ . \end{aligned} \tag{10}$$

Theoremthm1 The controller $\mathbf{u} = \boldsymbol{\alpha}_2(\boldsymbol{\zeta})$ stablises Eq. 5 and constitutes Eq. 6 if the following criteria are satisfied:

$$\frac{1}{2}\mathbf{P}\hat{\mathbf{A}} + \frac{1}{2}\hat{\mathbf{A}}'\mathbf{P} - \frac{1}{4}\mathbf{P}\hat{\mathbf{B}}\mathbf{R}^{-1}\hat{\mathbf{B}}'\mathbf{P} + \frac{1}{4\gamma^2}\mathbf{P}^2 + \mathbf{Q} = 0,$$
$$\mathbf{G}\hat{\mathbf{C}} = \hat{\mathbf{A}} + \frac{1}{2\gamma^2}\mathbf{P} + \frac{1}{4}\mathbf{P}\hat{\mathbf{B}}\mathbf{R}^{-1}\hat{\mathbf{B}}'\mathbf{P} + \frac{1}{4\gamma^2}\mathbf{I}. \tag{11}$$

where $\mathbf{P} > 0$ is a symmetric positive definite matrix.

Proof. Considering the function $V(\mathbf{x}) = \frac{1}{2}\mathbf{x}'\mathbf{P}\mathbf{x}$, then the HJI equation in Eq. 5 becomes:

$$HJI : \mathbf{x}'\mathbf{P}\hat{\mathbf{A}}\mathbf{x} + \frac{1}{4\gamma^2}\mathbf{x}'\mathbf{P}^2\mathbf{x} - \frac{1}{4}\mathbf{x}'\mathbf{P}\hat{\mathbf{B}}\mathbf{R}^{-1}\hat{\mathbf{B}}\mathbf{x} + \mathbf{x}'\mathbf{Q}\mathbf{x} \tag{12}$$

However, because all the terms in HJI are scalar values, it is possible to say $\mathbf{x}'\mathbf{P}\hat{\mathbf{A}}\mathbf{x} = \mathbf{x}'(\frac{1}{2}\mathbf{P}\hat{\mathbf{A}} + \frac{1}{2}\hat{\mathbf{A}}'\mathbf{P})\mathbf{x}$. Therefore, the HJI equation becomes:

$$HJI : \mathbf{x}'(\frac{1}{2}\mathbf{P}\hat{\mathbf{A}} + \frac{1}{2}\hat{\mathbf{A}}'\mathbf{P} - \frac{1}{4}\mathbf{P}\hat{\mathbf{B}}\mathbf{R}^{-1}\hat{\mathbf{B}}'\mathbf{P} + \frac{1}{4\gamma^2}\mathbf{P}^2 + \mathbf{Q})\mathbf{x}. \tag{13}$$

Accordingly, if $\mathbf{P}$ satisfies the first criterion in Eq. 11, then the HJI condition will be established automatically. Also, considering $W(\mathbf{x}, \boldsymbol{\zeta}) = \frac{1}{2}(\mathbf{x} - \boldsymbol{\zeta})'(\mathbf{x} - \boldsymbol{\zeta})$ concludes:

$$HJ : (\mathbf{x} - \boldsymbol{\zeta})'\hat{\mathbf{A}}\mathbf{x} + \frac{1}{2\gamma^2}(\mathbf{x} - \boldsymbol{\zeta})'\mathbf{P}\mathbf{x} \tag{14}$$
$$-(\mathbf{x} - \boldsymbol{\zeta})'\hat{\mathbf{A}}\boldsymbol{\zeta} - \frac{1}{2\gamma^2}(\mathbf{x} - \boldsymbol{\zeta})'\mathbf{P}\boldsymbol{\zeta} - (\mathbf{x} - \boldsymbol{\zeta})'\mathbf{G}\hat{\mathbf{C}}(\mathbf{x} - \boldsymbol{\zeta})$$
$$+\frac{1}{4}(\mathbf{x} - \boldsymbol{\zeta})'\mathbf{P}\hat{\mathbf{B}}\mathbf{R}^{-1}\hat{\mathbf{B}}'\mathbf{P}(\mathbf{x} - \boldsymbol{\zeta}) + \frac{1}{4\gamma^2}(\mathbf{x} - \boldsymbol{\zeta})'(\mathbf{x} - \boldsymbol{\zeta}),$$

which can be summarised as follows:

$$HJ : (\mathbf{x} - \boldsymbol{\zeta})'(\hat{\mathbf{A}} + \frac{1}{2\gamma^2}\mathbf{P} + \frac{1}{4}\mathbf{P}\hat{\mathbf{B}}\mathbf{R}^{-1}\mathbf{P} + \frac{1}{4\gamma^2}\mathbf{I} - \mathbf{G}\hat{\mathbf{C}})(\mathbf{x} - \boldsymbol{\zeta}). \tag{15}$$

Therefore, if the second criterion in Eq. 11 is satisfied, then the third condition for achieving Eq. 6 is satisfied. Furthermore, considering the Lyapunov function $S = \frac{1}{2}\boldsymbol{\zeta}'\boldsymbol{\zeta}$ for the system demonstrated in Eq. 8 then the time gradient of S can be written as:

$$\dot{S} = \boldsymbol{\zeta}'\dot{\boldsymbol{\zeta}} = \boldsymbol{\zeta}'(\hat{\mathbf{A}} + \frac{1}{2\gamma^2}\mathbf{P} - \mathbf{G}\hat{\mathbf{C}})\boldsymbol{\zeta}. \tag{16}$$

However, Eq. 16 can be written as follows according to the second criterion in Eq. 11:

$$\dot{S} = -\frac{1}{4}\boldsymbol{\zeta}'(\mathbf{P}\hat{\mathbf{B}}\mathbf{R}^{-1}\hat{\mathbf{B}}\mathbf{P} + \frac{1}{\gamma^2}\mathbf{I})\boldsymbol{\zeta} < 0 \ \forall \boldsymbol{\zeta} \neq 0\ , \tag{17}$$

that demonstrates the locally asymptotic stability of Eq. 8 according to the criteria in Eq. 11. Subsequently, if the conditions stated in Eq. 11 are satisfied, then all the criteria mentioned for achieving Eq. 6 are established and $\mathbf{u} = \boldsymbol{\alpha}_2(\boldsymbol{\zeta})$ will stabilise the system meanwhile guarantees the robust performance. ■

In conclusion, the control law $\mathbf{u} = -\frac{1}{2}\mathbf{R}^{-1}\hat{\mathbf{B}}'\mathbf{P}\boldsymbol{\zeta}$ will constitute the H_∞ conditions for Eq. 5 if $\boldsymbol{\zeta}$ is estimated by the following observer equation applying the matrices $\mathbf{P}$ and $\mathbf{G}$ determined from Eq. 11:

$$\dot{\boldsymbol{\zeta}} = \hat{\mathbf{A}}\boldsymbol{\zeta} + \boldsymbol{\alpha}_1(\boldsymbol{\zeta}) + \hat{\mathbf{B}}\boldsymbol{\alpha}_2(\boldsymbol{\zeta}) + \mathbf{G}(\mathbf{y} - \hat{\mathbf{C}}\boldsymbol{\zeta}) \tag{18}$$

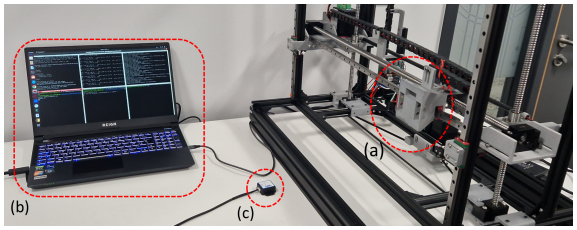

Fig. 2. The experimental setup for system identification and closed-loop system performance evaluation. (a) the mechanism head, (b) the station for test management and data acquisition, and (c) the accelerometer for vibration measurement.

6. RESULTS

This section presents the results obtained from implementing the output feedback H_∞ controller for vibration reduction. The test setup includes a Witmotion WT901C485 three-axis accelerometer to measure the acceleration transferred to the installation base as demonstrated in Fig.2. The vibration measurement frequency was set to 100 Hz to cover the target frequency range (0-50 Hz) for modal analysis. According to the model order determination presented in Section 4, the order of the system's state space model was determined as 12. Figure 3 demonstrates the power spectrum obtained from the measurement and the observer's output.

According to the results shown in Fig. 3, the power spectrum obtained from the H_∞ observer is accurately fitted to the spectrum for vibration measurements from the experiment in low frequencies. To evaluate the controller performance, two sets of experiments were conducted to examine the vibration measurement with and without the H_∞ controller Figure 4 shows the spectrogram results for the mechanism following the honeybee queen's trajectory without input shaping controller, with the state-feedback LQR controller, and the closed-loop response when the output feedback H_∞ determines the acceleration command to suppress the vibration.

According to the results presented in Fig. 4, applying the controller reduces the vibration intensity and establishes bounded outputs, demonstrating the closed-loop system's robust performance.

Although the experiment verifies the robust performance of the output feedback H_∞, it is worth comparing its performance with another control technique to evaluate its capability in regulating vibration for the AROBA system. The LQR method implemented in Rekabi-Bana et al. (2024) is considered for comparison.

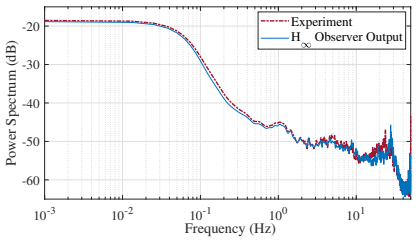

Fig. 3. Comparison results for vibration reduction with top-with LQR controller, bottom-with H_∞ controller

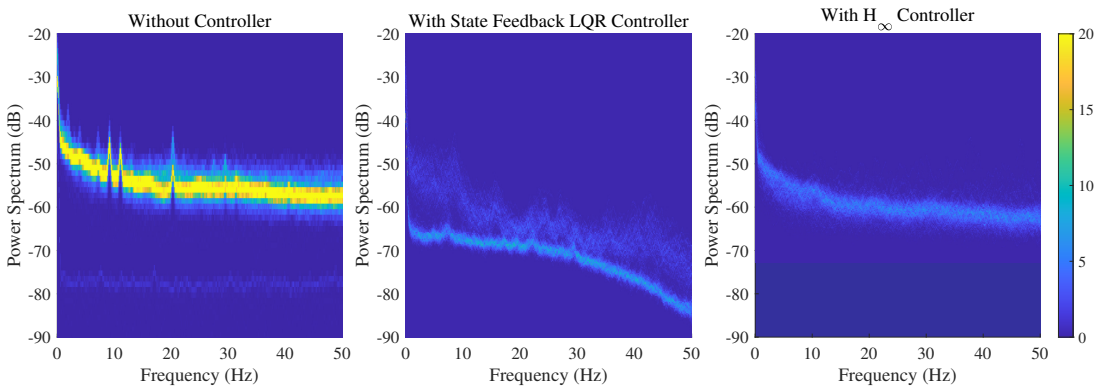

Fig. 4. Frequency Response of the system without the controller and with output feedback H_∞ input shaping controller.

According to the results presented in Rekabi-Bana et al. (2024) and in Fig. 4, although the state feedback controller reduces the vibration signal's power by 10 dB, it is evident that the modal response (particularly at peak frequencies) is the same with and without the controller. However, the output feedback H_∞ makes the modal response almost flat and suppresses the vibration signal's intensity, particularly at peak frequencies. In addition to the performance evaluation in the frequency domain, it is necessary to assess the tracking performance of the implemented system with output-feedback H_∞ for vibration reduction. The following figure demonstrates the tracking error and the position output of the mechanism's head to compare the system's performance with and without the implemented algorithm.

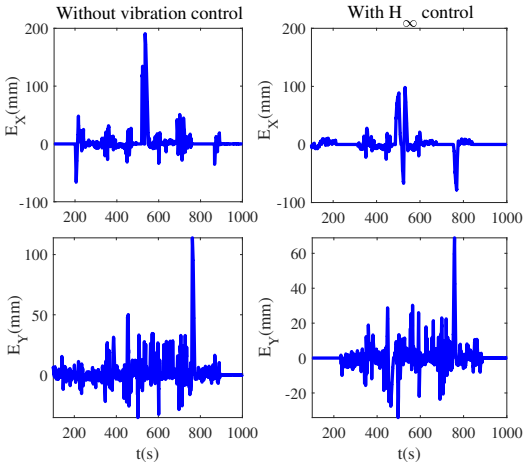

Fig. 5. Comparison results for the trajectory tracking error without the input shaping and with H_∞ controller

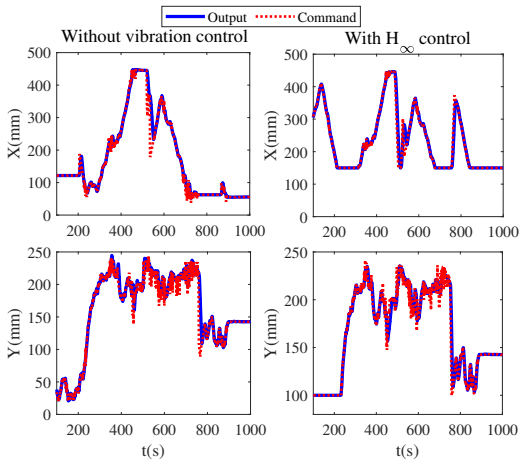

Fig. 6. Comparison results for the trajectory tracking results without the input shaping and with H_∞ controller

According to Fig. 5 and Fig. 6, although the H_∞ controller limits the acceleration command to suppress the vibration, the closed-loop system shows reasonable tracking accuracy which is an important criterion for the autonomous observation mechanism to follow the queen honeybee accurately during the data collection.

7. CONCLUSION

This paper proposes a robust vibration attenuation approach to suppress the AROBA system's vibration while it performs behavioural monitoring of the honeybee queen. A model with an order of about 12 is determined by applying the MOESP method to estimate the system's vibration intensity from the acceleration input. That model is employed for the H_∞ controller and observer. The experiment's results show that the observer can accurately estimate the vibration intensity. Accordingly, the closed-loop system demonstrates its performance by reducing the vibration signal's power level to -65 dB on average, which is 10 dB lower than the signal's level without the controller. Future research will address optimisation for the controller parameters and consider the effect of other practical elements such as input saturation, dead zone, and discrete integrator.

REFERENCES

Balaji, P. and Karthik Selva Kumar, K. (2021). Applications of nonlinearity in passive vibration control: a review. *Journal of Vibration Engineering & Technologies*.

Barmak, R., Stefanec, M., Hofstadler, D.N., Piotet, L., Schönwetter-Fuchs-Schistek, S., Mondada, F., Schmickl, T., and Mills, R. (2023). A robotic honeycomb for interaction with a honeybee colony. *Science Robotics*.

Blaha, J., Mikula, J., Vintr, T., Janota, J., Ulrich, J., Rouček, T., Rekabi-Bana, F., Fedotoff, L.A., Stefanec, M., Schmickl, T., et al. (2024). Effective searching for the honeybee queen in a living colony. In *2024 IEEE 20th International Conference on Automation Science and Engineering (CASE)*.

Dumanli, A. and Sencer, B. (2018). Optimal high-bandwidth control of ball-screw drives with acceleration and jerk feedback. *Precision Engineering*.

Favoreel, W., De Moor, B., and Van Overschee, P. (2000). Subspace state space system identification for industrial processes. *Journal of Process Control*.

Hrncir, M., Maia-Silva, C., and Farina, W.M. (2019). Honey bee workers generate low-frequency vibrations that are reliable indicators of their activity level. *Journal of Comparative Physiology A*.

Isidori, A. and Astolfi, A. (1992). Disturbance attenuation and h_∞ control via measurement feedback in nonlinear systems. *IEEE transactions on automatic control*, 37(9), 1283–1293.

Janota, J., Blaha, J., Rekabi-Bana, F., Ulrich, J., Stefanec, M., Fedotoff, L., Arvin, F., Schmickl, T., and Krajník, T. (2024). Towards robotic mapping of a honeybee comb. In *2024 International Conference on Manipulation, Automation and Robotics at Small Scales (MARSS)*.

Li, L., Zhang, Q., Zhang, T., and Zou, Y. (2023). Vibration suppression of ball-screw drive system based on flexible dynamics model. *Engineering Applications of Artificial Intelligence*.

Liu, X., Li, Y., Cheng, Y., and Cai, Y. (2023). Sparse identification for ball-screw drives considering position-dependent dynamics and nonlinear friction. *Robotics and Computer-Integrated Manufacturing*.

Łopuch, S. and Tofilski, A. (2017). Direct visual observation of wing movements during the honey bee waggle dance. *Journal of Insect Behavior*.

Lu, Z., Wang, Z., Zhou, Y., and Lu, X. (2018). Nonlinear dissipative devices in structural vibration control: a review. *Journal of Sound and Vibration*.

Pappalardo, C.M., Lök, Ş.İ., Malgaca, L., and Guida, D. (2023). Experimental modal analysis of a single-link flexible robotic manipulator with curved geometry using applied system identification methods. *Mechanical Systems and Signal Processing*.

Rekabi, F., Shirazi, F.A., Sadigh, M.J., and Saadat, M. (2020). Nonlinear h measurement feedback control algorithm for quadrotor position tracking. *Journal of the Franklin Institute*.

Rekabi-Bana, F., Saadat, M., Kalantaryardebily, N., Stefanec, M., Fedotoff, L.A., Pan, H., Krajník, T., Schmickl, T., and Arvin, F. (2024). Active vibration reduction for the autonomous observation mechanism. In *2024 IEEE Conference on Control Technology and Applications (CCTA)*.

Rekabi-Bana, F., Stefanec, M., Ulrich, J., Keyvan, E.E., Rouček, T., Broughton, G., Gündeğer, B.Y., Şahin, O., Turgut, A.E., Şahin, E., Krajník, T., Schmickl, T., and Arvin, F. (2023). Mechatronic design for multi robots-insect swarms interactions.

Romano, D., Donati, E., Benelli, G., and Stefanini, C. (2019). A review on animal–robot interaction: from bio-hybrid organisms to mixed societies. *Biological Cybernetics*.

Romano, D., Porfiri, M., Zahadat, P., and Schmickl, T. (2024). Animal–robot interaction—an emerging field at the intersection of biology and robotics. *IOP Journal of Bioinspiration & Biomimetics*.

Shirvani, H.K., Zeng, J.Q.C., and Erkorkmaz, K. (2022). Dynamic compliance attenuation in ball screw drives through model-based active damping of multiple vibration modes. *CIRP Annals*.

Soares Jr, D. and Serpa, A.L. (2022). An iterative state-space identification method with data correlation for mimo systems with measurement noise. *Journal of the Franklin Institute*.

Stefanec, M., Hofstadler, D.N., Krajník, T., Turgut, A.E., Alemdar, H., Lennox, B., Şahin, E., Arvin, F., and Schmickl, T. (2022). A minimally invasive approach towards "ecosystem hacking" with honeybees. *Frontiers in Robotics and AI*.

Stefanec, M., Oberreiter, H., Becher, M.A., Haase, G., and Schmickl, T. (2021). Effects of sinusoidal vibrations on the motion response of honeybees. *Frontiers in Physics*.

Ulrich, J., Stefanec, M., Rekabi-Bana, F., Fedotoff, L.A., Rouček, T., Gündeğer, B.Y., Saadat, M., Blaha, J., Janota, J., Hofstadler, D.N., Žampachů, K., Keyvan, E.E., Erdem, B., Şahin, E., Alemdar, H., Turgut, A.E., Arvin, F., Schmickl, T., and Krajník, T. (2024). Autonomous tracking of honey bee behaviors over long-term periods with cooperating robots. *Science Robotics*.

Van Overschee, P. and De Moor, B. (1994). N4sid: subspace algorithms for the identification of combined deterministic-stochastic systems. *Automatica*.

Yalçın, B.C. and Erkan, K. (2021). 3-dof zero power micro vibration isolation via linear matrix inequalities based on h and h2 control approaches. *Mechanical Systems and Signal Processing*.

Yang, H., Wang, Z., Zhang, T., and Du, F. (2020). A review on vibration analysis and control of machine tool feed drive systems. *The International Journal of Advanced Manufacturing Technology*.

Žampachů, K., Ulrich, J., Rouček, T., Stefanec, M., Dvořáček, D., Fedotoff, L., Hofstadler, D.N., Rekabi-Bana, F., Broughton, G., Arvin, F., et al. (2022). A vision-based system for social insect tracking. In *2nd International Conference on Robotics, Automation and Artificial Intelligence (RAAI)*.

Zhu, J., Zhang, T., Wang, J., and Li, X. (2016). Axial dynamic characteristic parameters identification of rolling joints in a ball screw feed drive system. *Proceedings of the Institution of Mechanical Engineers, Part C: Journal of Mechanical Engineering Science*.

Zhu, M., Bao, D., Sun, M., and Liu, Y. (2023). Tracking and vibration control with a parallel structure controller based on a flexible ball screw drive system. *Actuators*.